

**Screening correlators with chiral fermions**R. V. Gavai<sup>+</sup> and Sourendu Gupta<sup>+</sup>*Department of Theoretical Physics, Tata Institute of Fundamental Research, Homi Bhabha Road, Mumbai 400005, India*R. Lacaze<sup>‡</sup>*Service de Physique Theorique, CEA Saclay, F-91191 Gif-sur-Yvette Cedex, France*

(Received 10 March 2008; published 16 July 2008)

We study screening correlators of quark-antiquark composites at  $T = 2T_c$ , where  $T_c$  is the QCD phase transition temperature, using overlap quarks in the quenched approximation of lattice QCD. As the lattice spacing is changed from  $1/4T$  to  $a = 1/6T$  and  $1/8T$ , we find that screening correlators change little, in contrast with the situation for other types of lattice fermions. All correlators are close to the ideal gas prediction at small separations. The long distance falloff is clearly exponential, showing that a parameterization by a single screening length is possible at distances  $z \geq 1/T$ . The correlator corresponding to the thermal vector is close to the ideal gas value at all distances, whereas that for the thermal scalar deviates at large distances. This is examined through the screening lengths and momentum space correlators. There is strong evidence that the screening transfer matrix does not have reflection positivity.

DOI: [10.1103/PhysRevD.78.014502](https://doi.org/10.1103/PhysRevD.78.014502)

PACS numbers: 11.15.Ha, 12.38.Mh

**I. INTRODUCTION**

Current experiments at the Brookhaven RHIC and another to be started soon at the CERN LHC are engaged in creating and understanding the phase of matter called the quark gluon plasma. The existence of this phase was predicted by lattice QCD, and this technique has been used to study many properties of the plasma. In spite of this, much remains to be done. One of the major questions, that which concerns us here, is the nature of the interactions between quasiparticle excitations.

Decisive information on flavored quasiparticles has come from a recent study of the linkage between quantum numbers [1]. A rapid and clear change in the linkage between quantum numbers was seen across the QCD phase transition. In the high temperature phase flavor quantum numbers such as baryon number, charge, strangeness etc., are linked to each other in ways that suggest that the light flavored excitations at finite temperature QCD include quarks.

At the same time it is clear that the interactions between these quasiparticles cannot be small. At length scales of order  $1/T$ , the QCD coupling,  $g$ , is of order 1 [2], leading to well-known problems. For example, the Debye screening length of gluons is more complicated than one expects in perturbation theory [3] and contains pieces which are entirely nonperturbative [4]. The nonperturbative pieces have been isolated and studied on the lattice [5]. Interestingly, when one studies the screening of glueball-like quantities, i.e., spatial correlations of color singlet operators made out of gauge fields, then a surprising

simplicity arises above about  $1.25T_c$ . Taking two quantum number channels which can be constructed by a minimum of two and three gluon operators, the ratio of the screening masses is seen to be close to  $3/2$  [6].

There are parallels in the study of hadronlike screening correlators in the QCD plasma. Parity doubling was seen in the high-temperature phase of QCD in the first study of these correlators using staggered quarks [7]. Further, this first study already showed that the screening mass from the baryonlike correlator was  $3/2$  times the screening mass from some of the mesonlike correlators. A finite size scaling study using staggered quarks [8] showed that a particular combination of the vector and axial-vector mesonlike correlators was very close to the free-field theory (i.e., ideal gas) predictions. This behavior is generic, being seen in quenched [9] and dynamical QCD with two [10] and four [11] flavors of staggered quarks as well as with Wilson quarks [12]. Extrapolation to the continuum using staggered quarks [13] showed that the remaining screening masses approached their ideal-gas values. However, the correlators differed strongly from the ideal-gas correlators at small distances. This was also seen in a later study of screening correlators with Wilson quarks [14].

Overlap quarks [15] have the advantage of preserving all chiral symmetries on the lattice for any number of massless flavors of quarks [16]. This is in contrast to other formulations, such as Wilson's, which break all chiral symmetries, or the staggered, which break them partially. Since the number of pions and their nature is intimately related to the actually realized chiral symmetry on the lattice, one expects any realization of chiral quarks on the lattice to provide insight into this question.

In our earlier study of screening correlators using overlap quarks [17] with lattice spacing  $a = 1/4T$ , the correlation functions were found to decay exponentially at large

\*gavai@tifr.res.in

+sgupta@tifr.res.in

‡Robert.Lacaze@cea.fr

separation, and showed none of the fine structure that plague staggered and Wilson quarks. As a result, the screening mass was a good parametrization of the screening correlator at large distances. The screening masses in all channels were closer to the expected weak-coupling continuum limit for overlap quarks than staggered and Wilson. However, that from the (would be zero-temperature) scalar and pseudoscalar was lower by about 10% than the others.

In this paper we extract complete information on meson-like screening correlators by extending the analysis of [6,18] to overlap quarks. At the same time, we extend the analysis towards the continuum limit by using lattice spacings of  $a = 1/6T$  and  $1/8T$ . With these two inputs we are able to resolve all the currently outstanding questions on screening correlators. Parts of these results were presented in [19].

## II. SYMMETRIES

We study correlation functions of color singlet operators constructed with a quark and an antiquark—

$$C_\Gamma(z) = \langle M_\Gamma(0)M_\Gamma^\dagger(z) \rangle, \quad (1)$$

$$\text{where } M_\Gamma(z) = \frac{1}{N_t N_s^2} \sum_{xyt} \bar{\psi}(txyz)\Gamma\psi(txyz),$$

$\psi$  is a Dirac spinor,  $\Gamma$  is a Dirac matrix, the angular brackets denote averaging over gauge configurations and the quark bilinear  $M_\Gamma$  is projected to zero momentum in the slice orthogonal to  $z$  by the summation. By choosing different Dirac matrices,  $\Gamma$ , one explores different quantum numbers, and the usual nomenclature is explained in Table I. Note that the correlators projected on zero momentum ( $k_x = k_y = k_t = 0$ ) have mass dimension 3, and hence the quantity  $a^3 C(z)$  is dimensionless.

Since we work at finite temperature, the Dirac operator is defined with antiperiodic boundary conditions on  $t$  ( $1 \leq t \leq N_t$ ). We chose to impose periodic boundary conditions in the spatial directions ( $1 \leq x, y \leq N_s$  and  $1 \leq z \leq N_z$  with  $N_s \leq N_z$ ). Later we shall have occasion to use the aspect ratio  $\zeta = N_z/N_s$  (note that this is different from the often used aspect ratio  $N_s/N_t$ ). The sum over  $x, y$  and  $t$  in Eq. (1) accomplishes a projection on to zero total momentum in these three directions. Note that there is yet another aspect ratio,  $N_s/N_t$ , which needs to be large in the thermodynamic limit.

Because of the inequivalence of the spatial directions  $x$  and  $y$  with the Euclidean time direction  $t$  at finite temperature, a slice of the lattice orthogonal to the  $z$  direction differ at zero and finite temperature. These are part of the symmetries of the transfer matrix.<sup>1</sup> Therefore the classification

<sup>1</sup>The remaining symmetries are flavor symmetries. For staggered quarks the analysis is complicated [18] by the mixing of flavor and spacetime symmetries.

TABLE I. The break up of irreps under the successive breakings of the symmetries of the transfer matrix. The  $A_1^\pm$  components of the V/AV correspond to the  $t$  polarization and the  $E^\pm$  to the  $x$  and  $y$  polarizations. All states also carry a label for charge conjugation,  $C$ . This has been dropped in this paper since we consider only the  $C = 1$  states.

	$T = 0$		$T > 0$	
	continuum $O(3) \times Z_2(P)$	lattice $O_h$	continuum $O(2) \times Z_2(\mathcal{T})$	lattice $D_4^h$
S	$0^+$	$A_1^+$	$0^+$	$A_1^+$
PS	$0^-$	$A_1^-$	$0^-$	$A_1^-$
V	$1^+$	$F_1^+$	$0^-$	$A_1^-$
			$1^+$	$E^+$
AV	$1^-$	$F_1^-$	$0^+$	$A_1^+$
			$1^-$	$E^-$

of operators  $M_\Gamma$  differ at zero and finite temperature. This is described below and summarized in Table I.

At  $T = 0$  in the continuum one has the full rotational symmetry  $O(3)$  and the discrete symmetries of parity  $P$  and charge conjugation  $C$ . States corresponding to the irreducible representations (irreps) of  $O(3) \times Z_2(P) \times Z_2(C)$  are labeled by  $J^{PC}$ . On the lattice this group is broken to the discrete subgroup which is the cubic group  $O_h$ . The  $0^{PC}$  states (S/PS) become the  $A_1^{PC}$  of the cubic group and the  $1^{PC}$  states (V/AV) become the three dimensional irrep  $F_1^{PC}$  (sometimes called the  $T_1^{PC}$ ) [20]. The  $2^{PC}$  breaks into a three dimensional irrep called the  $F_2^{PC}$  (or  $T_2^{PC}$ ) and a two dimensional irrep called the  $E^{PC}$ .

For  $T \neq 0$ , the continuum theory has a  $O(2)$  rotational symmetry in the  $xy$  plane and a  $Z_2(\mathcal{T})$  symmetry (Euclidean time reversal) in the Euclidean time direction. This constitutes the cylinder group,  $O(2) \times Z_2(\mathcal{T})$ , which is a subgroup of  $O(3) \times Z_2(P)$ . On the lattice this is broken to the dihedral group  $D_4^h = D_4 \times Z_2(\mathcal{T})$  (where  $D_4$  is the group of symmetries of a square), which is also a subgroup of  $O_h$ , as is to be expected [21].

The  $J^{PC}$  irreps of  $T = 0$  break up into  $M^{TC}$  irreps at finite temperature, where  $M = J_z$  (since the cylinder group is Abelian, its complex irreps are one-dimensional). The reduction under the lattice symmetries is shown in Table I. The group theory is the most general. However, it does not restrict special cases in which some of the independent representations may become identical for dynamical reasons. We discuss these next.

Note that the  $T = 0$  vector breaks into two irreps for  $T > 0$ . This group theory need not contradict our intuition that at sufficiently low, but finite, temperature, the screening spectrum should be very similar to the  $T = 0$  hadron spectrum, and therefore the thermal  $0^-$  and  $1^+$  should be nearly degenerate. When the screening mass,  $\mu$ , is sufficiently small (i.e.,  $\mu/T \gg 1$ ), then the effect of the boundaries must be exponentially small. The approximate symmetry  $O_h$  is broken to  $D_4^h$  via terms that are exponen-

tially small, leading to near-degeneracy of the components of  $T_1$  (the splitting can only be observed with exponentially large statistics). After all, the situation is not different from the  $T = 0$  theory defined with various different boundary conditions—they are equivalent as long as  $mL \gg 1$  where  $L$  is the size of the box in which the theory is defined.

However, this resolution raises another problem—can the masses of the two  $0^-$  states, one obtained from the reduction of the PS and the other from the V be equal? If the mass of the latter becomes equal to that of the  $1^+$  at low temperature, do we predict that the PS and V states must be degenerate, contrary to previous knowledge? The answer must be negative, the resolution being that the  $0^-$  coming from the V cannot have overlap with the eigenvector of the transfer matrix with the smallest eigenvalue. This argument predicts that the screening masses in the V and PS channel (and similarly in the S and AV channels) must be different, although the naive transfer matrix argument gives a different result.

The correlator identities

$$C_S(z) = -C_{PS}(z) \quad C_V(z) = -C_{AV}(z) \quad (2)$$

can be proven for overlap quarks by neglecting the effects of instantons. This shows parity doubling. As can be seen from Table I, there is no group theoretical reason behind parity doubling. If there were, then that would force chiral symmetry at all  $T$ .

Gauge field configurations which give rise to chiral zero modes of the overlap Dirac operator (called instantons) have interesting consequences. Since these modes are localized, one recovers translation invariance by averaging over many such configurations. At high temperatures it is observed that these configurations are rather improbable. Hence, to take their effects properly into account one must either use truly astronomical statistics or consider the zero momentum correlators,  $\chi_\Gamma$ , i.e., correlators such as those in Eq. (1) summed over  $1 \leq z \leq N_z$ . These have been analyzed in [17] and various identities were checked. One should note that any configuration with a chiral zero mode breaks the identity  $C_S(z) = -C_{PS}(z)$ . Configurations with zero modes of both positive and negative chirality break the identity  $C_V(z) = -C_{AV}(z)$ . Thus, generic ensembles of gauge configurations including instantons would realize only the irreps in Table I. Parity doubling, represented in Eq. (2) involves the disappearance of chiral zero modes. It has been noted [17] that these do not disappear at the QCD phase transition but only gradually with increasing  $T$ . Hence parity doubling in the high temperature phase is an approximate statement, and extremely high statistics studies will be able to see the breaking of this approximate symmetry.

### III. FREE OVERLAP QUARKS

The overlap Dirac operator ( $D$ ) can be defined [22] in terms of the Wilson-Dirac operator ( $D_w$ ) by the relation

$$D = 1 - D_w(D_w^\dagger D_w)^{-1/2}. \quad (3)$$

When the gauge fields are translation invariant,  $D_w$  can be diagonalized in the Fourier basis. In free field theory, one can write

$$D_w = c + i\gamma_\mu b_\mu, \quad \text{where } c = 1 + s - \sum_\mu \sin^2(p_\mu/2), \\ b_\mu = -\sin p_\mu, \quad (4)$$

where  $s$  is the (negative) mass parameter, and, at finite  $T$ , the momenta are  $p_0 = 2\pi(n + 1/2)/N_t$  and  $p_i = 2\pi n/N_s$ . Since  $D^\dagger D = c^2 + b \cdot b$ , and therefore diagonal, the overlap Dirac operator is

$$D = \alpha + i\gamma_\mu \beta_\mu, \quad \text{where } \alpha = 1 - \frac{c}{\sqrt{c^2 + |b|^2}}, \\ \beta_\mu = \frac{b_\mu}{\sqrt{c^2 + |b|^2}}, \quad (5)$$

where  $|b|^2 = b \cdot b$ . Clearly the eigenvalues of  $D$  lie on the unit circle centered on the real axis at  $(1, 0)$ .

Writing the eigenvalues of  $D_w$  as  $\lambda(D_w) = r \exp(i\theta)$ , with  $r^2 = c^2 + |b|^2$  and  $\theta = \tan^{-1}(|b|/c)$ , it is easy to see that the eigenvalues of  $D$  are given by  $\lambda(D) = \rho \exp(i\phi)$  where  $\rho^2 = 2(1 - \cos\theta) = 2(1 - c/r)$  and  $\phi = (\pi - \theta)/2$ . It is easy to check that in the limit  $N_t \rightarrow \infty$  the minimum eigenvalue is obtained by taking  $p_0 = \pi/N_t$  and  $p_i = 0$ . This gives

$$\rho = \frac{\pi}{(1+s)N_t} + \mathcal{O}\left(\frac{\pi}{N_t}\right)^3 \quad (6)$$

$$\phi = \frac{\pi}{2} + \mathcal{O}\left(\frac{\pi}{N_t}\right). \quad (7)$$

The factor of  $1 + s$  in the denominator is usually absorbed into a redefinition of the fermion fields, thus giving the correct Matsubara frequency in the continuum limit.

A massive overlap operator,  $D(m)$ , and the corresponding quark propagator,  $G(m)$ , are defined by

$$D(m) = m + (1 - m/2)D, \quad \text{and} \quad G(m) = K^{-1}(m), \\ \text{where } K(m) = [1 - D/2]D^{-1}(m), \quad (8)$$

and  $m$  is the bare quark mass in lattice units [22]. The massive overlap propagator can, therefore, be written in the form

$$G(p; m) = f(p; m) + i\gamma_\mu h_\mu(p; m),$$

$$\begin{aligned} \text{where } f(p; m) &= \left(1 - \frac{\rho}{2} \cos\phi\right) \left(1 + \frac{m}{2}\right) \cos\phi \\ &\quad + \rho \left(1 - \frac{m}{2}\right) \sin^2\phi, \\ h_\mu(p; m) &= \left[ \left(1 + \frac{m}{2} \cos\phi\right) \rho \right. \\ &\quad \left. - \left(1 - \frac{m}{2} \cos\phi\right) \left(1 - \frac{\rho}{2} \cos\phi\right) \right] \\ &\quad \times \sin\phi \beta_\mu. \end{aligned} \quad (9)$$

As  $m \rightarrow 0$ , we recover the usual massless propagator.

The screening correlator at external momentum  $q$  is then given by

$$C_\Gamma(q) = \sum_p \text{tr} G(p+q; m) \Gamma G^\dagger(p; m) \Gamma. \quad (10)$$

After performing the traces, one finds

$$C_\Gamma(q) = 4 \sum_p [f(p+q; m) f(p; m) + \Gamma_{\mu\nu} h_\mu(p+q) h_\nu(p)], \quad (11)$$

where the tensor  $\Gamma_{\mu\nu}$  is  $g_{\mu\nu}$  for S and  $2g_{\mu\lambda}g_{\nu\lambda} - g_{\lambda\lambda}g_{\mu\nu}$  for the  $\lambda$  polarization of V. The tensors  $\Gamma_{\mu\nu}$  for the PS and AV satisfy the correlator identities for overlap quarks. Define  $C_V$  to be the sum over three polarizations of the vector, then with the Euclidean metric one finds  $T_{\mu\nu} =$

$-g_{\mu\nu} - 2g_{zz}$ . As a result,

$$C_V(q) + C_S(q) = -12 \sum_p g_z(p+q) g_z(p), \quad (12)$$

which is generically nonzero.

In Fig. 1 we show some of the results of a numerical computation of some of the mesonlike correlators in free field theory on lattices of various sizes. One sees a gradual convergence of the results when plotted in terms of the scaling variables  $zT = az/N_\tau$  and  $C(zT)/T^3 = a^3 C(az/N_\tau)/N_\tau^3$ . Several features of the free field theory are interesting enough that we list them explicitly.

- (1) The correlator identities of Eq. (2) are satisfied. This is expected, since free field theory has no topological features which lead to localized zero modes. As noted before, these identities are stronger than the general feature expected from the group theoretical analysis, since they allow us to equate the  $A_1^+$  coming from PS to the  $A_1^-$  coming from the S, etc.
- (2) The correlators in the  $E^+$  and  $A_1^-$  irreps coming from the V have completely different behavior. Consistent with this, the  $E^-$  and the  $A_1^+$  correlators coming from the AV are quite different from each other. However, the  $E^\pm$  and the  $A_1^\pm$  are identical.
- (3) The  $A_1^-$  correlator from the V changes sign at  $z \simeq 2/T$ . The point at which the change of sign occurs is almost independent of  $N_z$  and  $N_{x,y}$ . This is clear evidence that a three dimensional effective theory

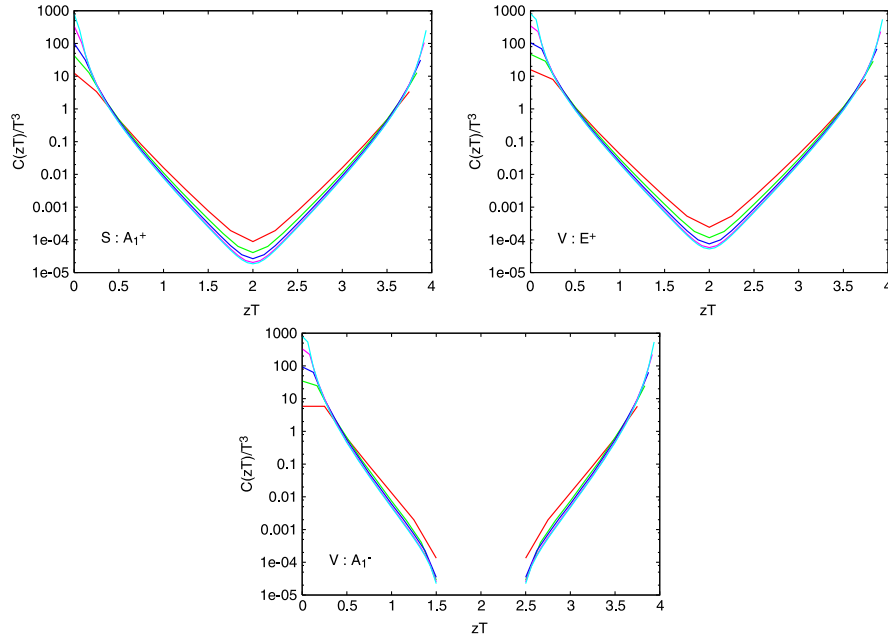


FIG. 1 (color online). Correlators computed in a free field theory of overlap quarks on lattice sizes  $4 \times 10^2 \times 16$ ,  $6 \times 14^2 \times 24$ ,  $8 \times 20^2 \times 32$ ,  $12 \times 30^2 \times 48$ , and  $16 \times 40^2 \times 64$ . The  $A_1^+$  correlator coming from S (first panel), the  $E^+$  correlator coming from V (second panel) and the  $A_1^-$  correlator coming from V (third panel) are shown. The value of  $N_\tau$  increases from top to bottom at  $zT = 2$ . The missing segments of the correlators in the last case correspond to the negative sign.

which describes these screening correlators cannot have reflection positivity.

- (4) The  $A_1^\pm$  coming from the V and AV are not degenerate with the  $A_1^\pm$  coming from the PS or the S, in agreement with the analysis of the previous section.
- (5) The  $A_1^\pm$  correlators from the PS and S are identical to the  $E^\pm$  correlators from the V and AV. There is no group theoretical reason for this, and we shall examine later whether this holds in the interacting theory.

#### IV. COMPUTATIONAL DETAILS

Our numerical work was done in quenched QCD with overlap valence quarks. We have computed all 8 components of the correlators (one each for S and PS and three polarizations each for the V and AV). Extensive finite size scaling studies were reported earlier [17] on lattices with  $a = 1/4T$ . We have extended this finite size scaling study here, but the main emphasis is on studying the variation with lattice spacing and taking the continuum limit. To this end we have used  $a = 1/6T$  and  $1/8T$ , at the temperature  $T = 2T_c$ , where  $T_c$  is the critical temperature for pure SU(3) gauge theory.

The computation of propagators using the overlap Dirac operator of Eq. (5) needs a nested set of two matrix inversions for its evaluation (each step in the numerical inversion of  $D$  involves the inversion of  $D_w^\dagger D_w$ ). This squaring of effort makes a study of QCD with dynamical overlap quarks very expensive. As before, we therefore chose to work with quenched overlap quarks.

We generated quenched QCD configurations at temperatures of  $T/T_c = 2$  on  $4 \times 10^2 \times 16$ ,  $6 \times 14^2 \times 24$  and  $8 \times 18^2 \times 32$  lattices (see Table II). The corresponding couplings are respectively  $\beta = 6.0625$ ,  $6.3384$  and  $6.55$ . Note that these are the known critical couplings on  $N_t = 8$ ,  $12$  and  $16$  lattices. For the latter, no infinite volume extrapolation was available, unlike the first two. Our choice was motivated by the 2-loop  $\beta$ -function, and consistency with the finite volume results. In each case, the configurations were separated by 1000 sweeps of a Cabibbo-Marinari update.

For the matrix  $M = D_w^\dagger D_w$ , and a given source vector  $b$ , we computed  $y = M^{-1/2}b$  by using the Zolotarev algo-

rithm [23]:

$$M^{-1/2}b = \sum_{l=1}^{N_O} \left( \frac{c_l}{M + d_l} b \right), \quad (13)$$

where the coefficients  $c_l$  and  $d_l$  are computed with Jacobi elliptic functions once one has the order of approximation  $N_O$  and the ratio  $\kappa = \mu_{\max}/\mu_{\min}$  where  $\mu_{\max}$  and  $\mu_{\min}$  are the boundaries of the domain where we apply the approximation. In our implementation of the algorithm [24], we first compute the lowest and highest eigenvalues of  $M$  and then choose  $\mu_{\max}$  and  $\mu_{\min}$  so that the domain of applicability of the Zolotarev approximation is 10% larger than the domain spanned by the eigenvalues. The order  $N_O$  is defined by requiring a precision  $\epsilon/2$  for the approximation of  $1/\sqrt{z}$  in the entire domain. With these parameters, one calculates the approximation in Eq. (13) by a multishift CG-inversion at the precision  $\epsilon/2$ .

On each gauge configuration we computed  $G$  on 12 point sources (3 colors and 4 spins) for 8 quark masses from  $m/T_c = 0.008$  to  $0.8$  using a multimass inversion of  $D^\dagger D$ . The (negative) Wilson mass term in  $D_w$ , i.e.,  $1 + s$  in Eq. (4), which is an irrelevant regulator, was set to  $1.8$ . The tolerance ranged from  $\epsilon = 10^{-5}$  to  $10^{-7}$  in the inner CG and  $10^{-3}$  to  $10^{-5}$  in the outer CG, with most of the work done using the larger values of  $\epsilon$ . We remark on the choice in a later section. Typical  $N_O$  needed was about 7–8.

For most configurations we found that the spectrum of  $D^\dagger D$  starts well away from zero. However, very occasionally (one each for  $N_t = 4$  and  $8$ ) we found a zero mode, i.e., an unpaired eigenvalue  $\leq 10^{-2}$ . As discussed in the literature, such zero modes have to be subtracted off to obtain averages of physical quantities such as the correlation functions. We showed elsewhere that our determination of the eigenvectors and eigenvalues is precise enough that we can subtract out the zero mode contribution in the chiral condensate. The resultant subtracted condensate (or correlators) is well within the statistical distribution of the measurement obtained in the sample without zero modes, at all the couplings and lattice sizes studied. We therefore chose not to include the zero mode contributions below. Furthermore, we show below results for our lowest quark mass  $m/T_c = 0.008$ , as the main features are essentially quark mass independent.

## V. RESULTS

### A. Symmetry realization

We have checked that the sum of the S and PS correlators vanishes within errors in all our measurements, in agreement with the correlator identities for overlap quarks. For the V and AV correlators we checked that the difference of the  $x$  and  $y$  polarization correlators vanish within errors, thus verifying that they lie in the same irrep of the symmetry group, as indicated by Table I.

In Fig. 2 we show the screening correlator obtained from various polarizations of the V. The  $t$ -direction polarization

TABLE II. Coupling  $\beta$  for temperature  $2T_c$ , the lattice size, and the number of configurations (separated by 1000 sweeps) used for analysis ( $N$ ).

$\beta$	Lattice Size	$N$
6.0625	$4 \times 10^2 \times 16$	19
6.3384	$6 \times 14^2 \times 24$	20
6.55	$8 \times 18^2 \times 32$	26
6.0625	$4 \times 12^3$	23
6.3384	$6 \times 14^3$	16

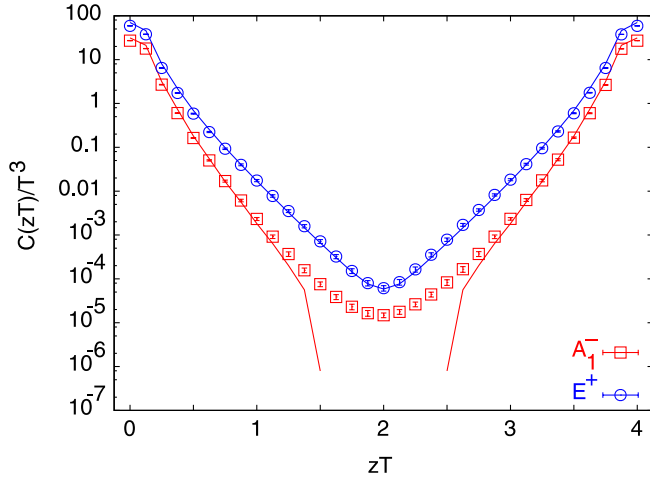


FIG. 2 (color online). The  $A_1^-$  and the  $E^+$  correlators coming from the V correlator on an  $8 \times 18^2 \times 32$  lattice at  $T = 2T_c$ . Also shown are the results of a free field theory (FFT) computation.

gives the  $A_1^-$  and the  $x$  and  $y$  directions give the  $E^+$ . In the figure we show the correlator from the sum of the  $x$  and  $y$  polarizations. We also show the corresponding correlator obtained from a free field theory (FFT) computation. Note the close agreement between the  $E^+$  correlator in the quenched theory and the FFT results, over 6 orders of magnitude change in the correlator. We will examine this in more detail later.

The disagreement between the FFT and the full theory for the  $A_1^-$  correlator shown in Fig. 2 requires further analysis. When the tolerance in the fermion inversion was decreased, the  $E^+$  correlator changed only marginally, whereas the  $A_1^-$  correlator changed sign at  $zT > 3/2$  on some gauge configurations. However, further work is required to check whether these correlators also turn negative as the tolerance is decreased further.

In the past the sum of the three polarizations of the  $T = 0$  vector have been analyzed together. Strictly speaking, this is incorrect, since it mixes the  $E^\pm$  and  $A_1^\mp$  irreps. However, the screening correlator in the latter irrep is almost an order of magnitude smaller than that in the former. As a result, the screening masses extracted by the older method is a fairly accurate measure of the screening mass in the  $E^\pm$  channel. In fact, we find that the screening mass from the  $E^+$  correlator at  $N_t = 8$  is  $a\mu_{E^+} = 0.798(4)$  whereas that from the mixed representation is  $a\mu_V = 0.816(4)$ . The two screening masses are compatible with each other at the  $3\sigma$  level.

With this caveat in mind, in the remainder of this paper we shall report results obtained with the older method of analysis, where the V correlator sums over all the polarizations. It has the advantage that the results are directly comparable with earlier results, and is not far removed from the quantitatively correct results which would be obtained by following the theoretically correct method.

## B. Correlations as functions of spatial separation

In Fig. 3 we compare the measured correlation functions in the S and V channels. It is noteworthy that the V correlator agrees rather well with the ideal-gas correlation functions from  $z = 0$  all the way to  $N_z/2$ , when the correlator itself falls by 6–7 orders of magnitude. To make this spectacular point more forcefully, we have plotted in Fig. 4 the ratio of the measured correlator with the ideal gas. It is clear that the V ( $E^+$ ) correlator differs from the ideal gas by no more than 10%–20% everywhere except (possibly) near the center of the lattice.

The situation is somewhat different for the S ( $A_1^+$ ) correlator. This agrees well with the ideal gas up to a distance  $z \approx 1/T$ . At distances larger than this, the S channel correlator falls significantly slower than the ideal-gas result (Fig. 3). This is shown again in Fig. 4, where it becomes clear that the ratio of the correlators changes by a factor of about 5 when the correlators themselves have changed by about 6 orders of magnitude.

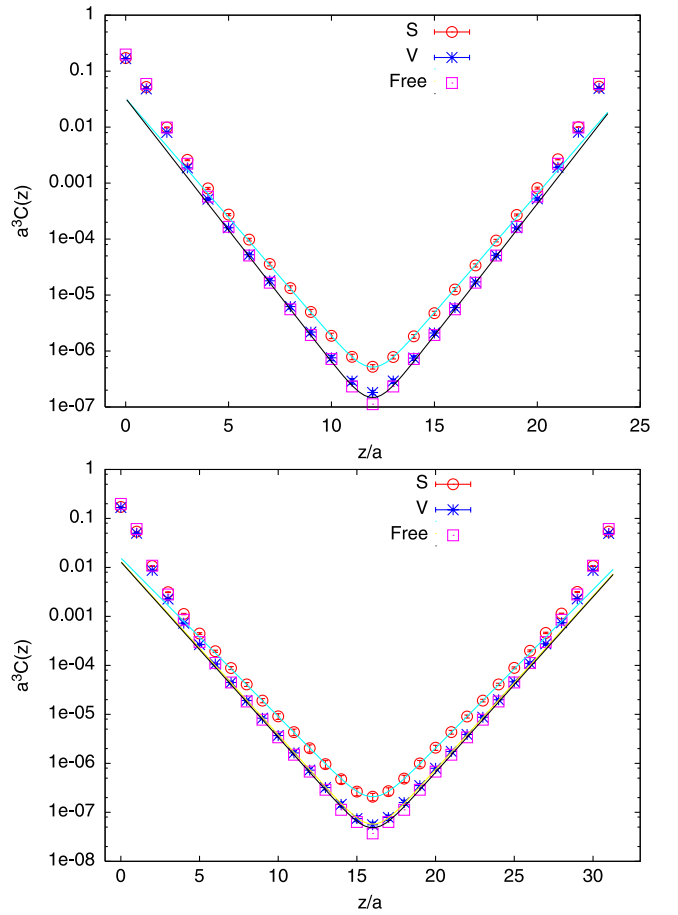


FIG. 3 (color online). Screening correlators in the S and V channels compared with the corresponding ideal-gas results on a  $6 \times 14^2 \times 24$  lattice (first panel) and an  $8 \times 18^2 \times 32$  lattice (second panel) at  $T = 2T_c$ . The lines are single cosh fits.

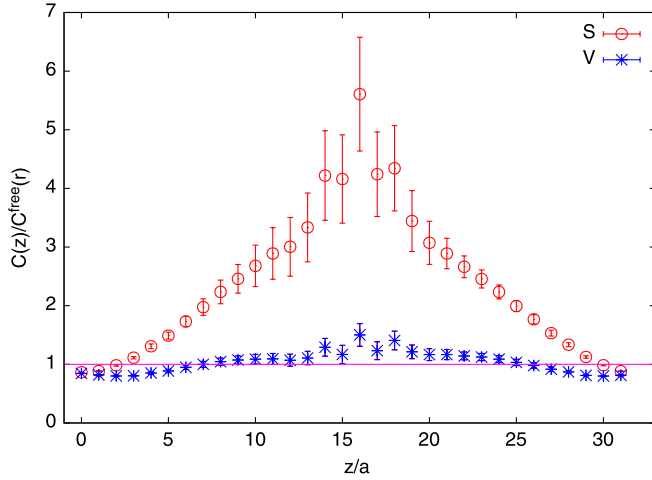


FIG. 4 (color online). The ratio of the measured and ideal-gas screening correlators in the S and V channels.

### C. Correlations as functions of momentum

In some applications the momentum space correlator is a more direct input, giving emphasis to the small  $z$  region. Our lattice data can be exhibited in momentum space by a Fourier transformation of the separation  $z$ . The periodic boundary conditions give rise to a Brillouin zone structure as usual, and only momenta in the range  $0 \leq k_z \leq \pi TN_t$  are independent.

We show the momentum space correlators in Fig. 5. It turns out that the ideal-gas result needs to be multiplied by a constant (independent of  $k_z$ ) in order to describe the data well. However, after this normalization, which we choose to fix the correlator at  $k_z = \pi TN_t$ , the shapes of the correlators are in rough agreement with the ideal-gas results, except at small  $k_z$ . From Fig. 5 another interesting feature which is visible is that the correlators at two different lattice spacings,  $a = 1/6T$  and  $1/8T$ , after the scaling by  $a^3$ , show no significant dependence on lattice spacing at  $k_z = \pi/4a, \pi/2a, 3\pi/4a$ , and  $\pi/a$ . However, there are small differences visible at low momenta,  $k_z < \pi T$ , for both the S and V correlators. With decreasing  $a$ , these residual  $a$ -dependent effects go in the direction of slightly improving the agreement with free field theory for V, and of making matters slightly worse for S.

The small disagreements with free field theory can be better exhibited by displaying the ratio of the correlator and its ideal-gas counterpart-  $C_\Gamma(k_z)/C_\Gamma^{\text{free}}(k_z)$ . These ratios are shown in the V and S channels for the  $8.18^2.32$  lattice in Fig. 6. The ratio shows clear structure. Near the center of the Brillouin zone,  $k_z \approx 4\pi T$ , the ratios go to a momentum independent constant. However, this constant is different from unity, and also different in the two channels. For  $k_z < 2\pi T$  the ratio is clearly momentum dependent. In the S channel, the ratio decreases with  $k_z$  whereas in the V channel it increases.

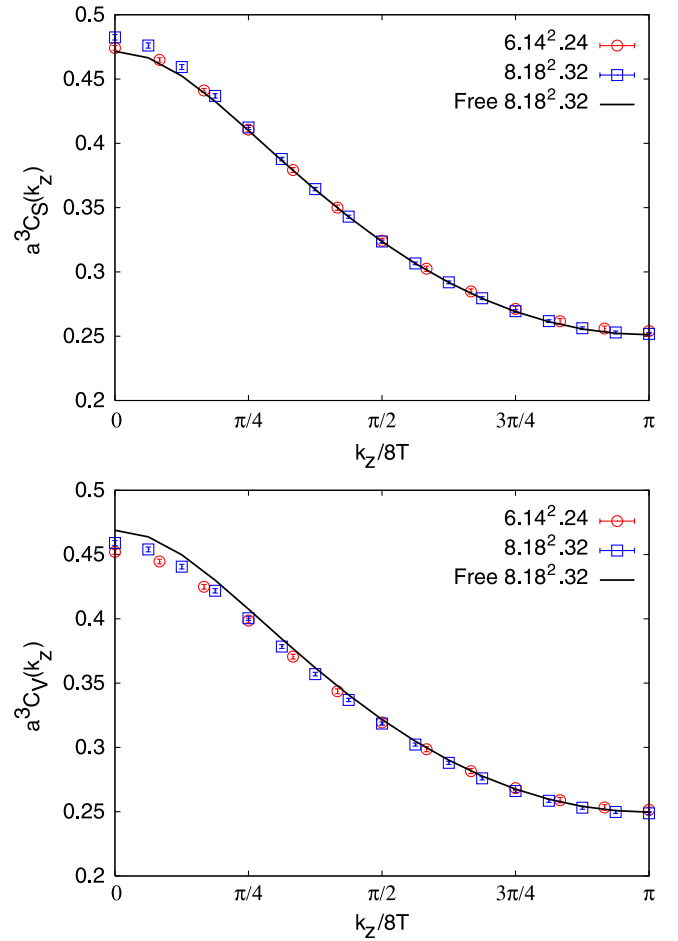


FIG. 5 (color online). Momentum space correlators at two different lattice spacings compared with the ideal-gas results, normalized to fit the high-momentum data, for the S (first panel) and V (second panel) channels.

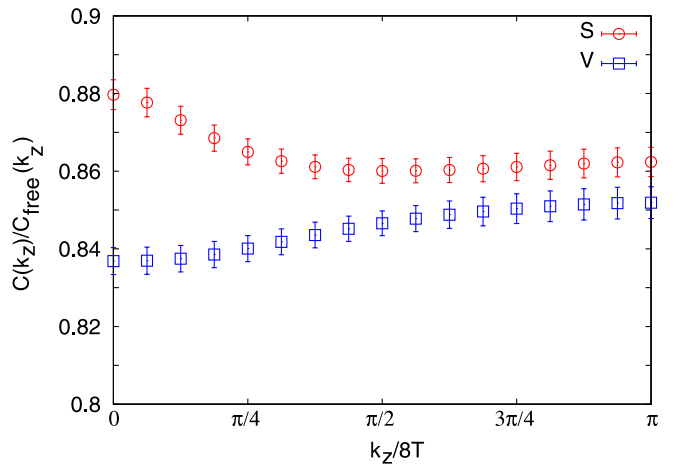


FIG. 6 (color online). The ratio of the measured and ideal-gas screening correlators in the S and V channels, on the  $8.18^2.32$  lattice.

### D. Screening masses

One can extract screening masses from the correlators in two different ways. One is by fitting a single cosh to the long distance part of the screening correlator. The other method is to use the ratio  $C(z)/C(z+1)$  and the assumption that at distance between  $z$  and  $z+1$  is described by a single cosh to extract a distance dependence effective mass,  $m(z)$ . If there is a clear plateau in the effective mass as a function of  $z$ , which agrees with the fitted value, then one could reliably talk of a screening mass and its value.

In Fig. 7 we exhibit the result of such a test. It is clear that there is a stable plateau over almost half the available distances, and the local mass in this region ( $z > 1/T$ ) agrees well with the results of a fit over the same range. This is quite different from earlier studies of staggered and Wilson quarks, where a stable plateau in the local masses was not observed. Note also the need for aspect ratios  $\zeta = N_z/N_s > 1$  in order to stabilize the local masses at their asymptotic value.

Notice the nonmonotonicity of the local masses at the smallest distance. If the correlation function could be expressed in the spectral form—

$$C(z) = \sum_i A_i [\exp(-m_i z) + \exp(-m_i \{N_z - z\})], \quad (14)$$

with all the  $A_i \geq 0$ , i.e., the correlation function came from a transfer matrix satisfying reflection positivity, then the local masses would be a nonincreasing function of distance for  $z < N_z/2$ . Clearly, therefore, the data shows that this condition is violated. Such behavior has been observed with both staggered and Wilson quarks earlier. Note also the lack of convexity of the screening correlators in Fig. 3, which is also a consequence of the violation of reflection positivity.

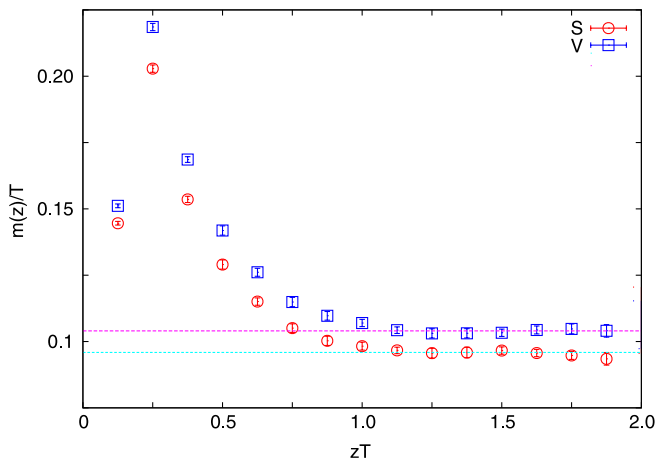


FIG. 7 (color online). Effective masses extracted on the  $8 \times 18^2 \times 32$  lattice, compared with the results of the fits to a single cosh indicated by the horizontal lines.

In Fig. 8 we plot the ratio of screening masses extracted in quenched QCD to that in a free field theory of overlap quarks on the same lattice,  $\mu/\mu_{\text{free}}$ , as a function of  $1/N_t^2 \propto a^2$  at fixed  $T = 2T_c$ .  $\mu_{\text{free}}$  was also obtained by both fitting the free correlator and applying the local mass technique to the free correlator in the same  $z$ -interval as for the interacting case. The results presented are for the  $z$  range of 9–14 (8–12) for  $N_t = 8(6)$ . The results are stable for small variation of this  $z$ -range. The values of the screening masses are collected in Table III. In the V channel the ratio is consistent with unity. In the S channel, however, the ratio differs from unity at the 95% confidence level but is almost independent of the lattice spacing.

We have shown results for two values of the aspect ratio,  $\zeta = 1$  and 1.7. At the smallest lattice spacing we have only  $\zeta = 1.7$ . It would be useful to extend these computations to larger  $\zeta$ . In view of our results, it is interesting to ask whether it is possible that at some larger value of  $N_t$  there is a cross over to a regime where  $\mu_S$  is closer to  $\mu_{\text{free}}$ . If such were the case, then one should be able to identify the

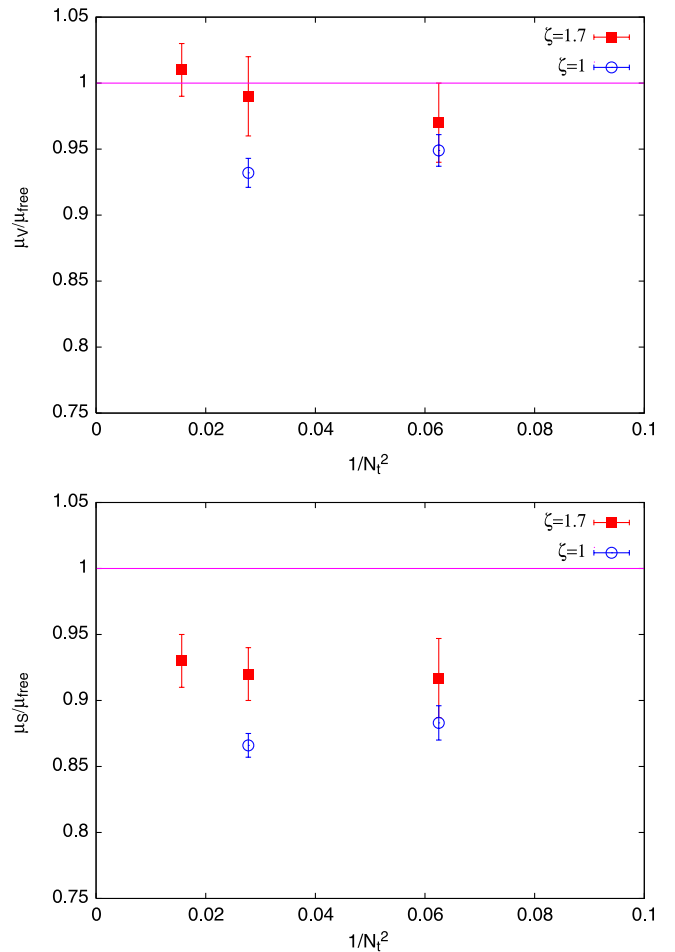
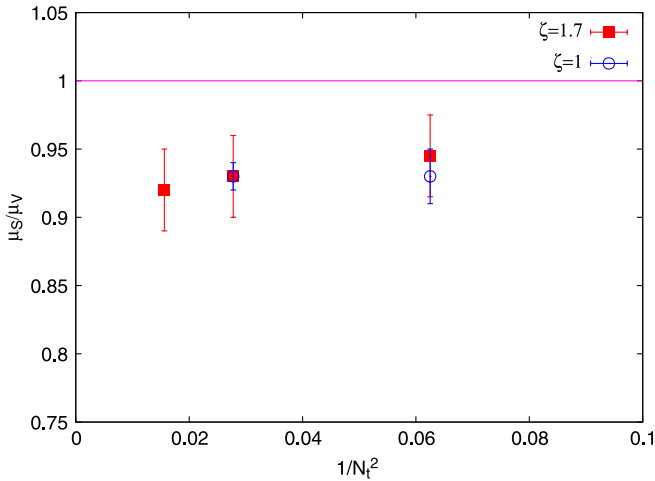


FIG. 8 (color online). The ratio of the screening mass in quenched QCD to that in a theory of free overlap quarks on the same lattice for the S and V channels at  $T = 2T_c$ . Results for two aspect ratios,  $\zeta = 1$  and 1.7, are shown.

TABLE III. Screening masses in lattice units for various lattice sizes at  $T = 2T_c$ .

Lattice size	$a\mu_S$	$a\mu_V$	$a\mu_{\text{free}}$
$4 \times 10^2 \times 16$	1.41(1)	1.49(1)	1.55(1)
$6 \times 14^2 \times 24$	1.00(4)	1.07(4)	1.08(1)
$8 \times 18^2 \times 32$	0.77(3)	0.84(3)	0.83(1)
$4 \times 12^3$	1.52(1)	1.63(1)	1.72(1)
$6 \times 14^3$	1.05(1)	1.13(1)	1.21(2)


 FIG. 9 (color online). The ratio of the screening mass in the S and V channels in quenched QCD are shown as a function of  $1/N_f^2 \propto a^2$  for  $T = 2T_c$ . Results for two aspect ratios,  $\zeta = 1$  and  $1.7$ , are shown.

physics of such a cross over. There is only one such piece of physics, and that is the scale of nonlocality of the overlap Dirac operator. This has been studied in [25], where it was shown that the scale of nonlocality varies smoothly towards zero as the lattice cutoff decreases. This allows us to rule out a crossover from the observed behavior of  $\mu_S$  to trivial physics.

A direct comparison of the screening masses in the S and V channels is shown in Fig. 9. Although the errors are large, one sees a trend towards increase in the ratio with increasing  $\zeta$ . From this figure it is clear that these two masses differ from each other at the 95% confidence limit at the smallest lattice spacing that we use, and show no tendency to move towards equality. Since the ratio  $\mu_S/\mu_V$  is within 5% of unity, an explanation within a weak coupling expansion seems possible. However, there is no such explanation available at this time.

## VI. SUMMARY

We have performed a group theoretical analysis of the screening transfer matrix at finite temperature. Quark bilinear operators, in the  $C = +1$  sector, which are classified

as S, PS, V, and AV at zero temperature can be decomposed at finite temperature as shown in Table I. The thermal state  $A_1^-$  is obtained in the decomposition of both the PS and V. Parity doubling is not a consequence of the group theory, but arises dynamically. Some identities which can be proven for the topologically trivial sector of overlap quarks, Eq. (2), show parity doubling. We presented an argument that if the PS and V are not to be degenerate at low temperatures, then they cannot be degenerate at any temperature. The theory of free overlap quarks is consistent with the converse, since it gives a degeneracy between the PS and V at all temperatures. As a result, this theory cannot be an accurate representation of all aspects of QCD at finite temperature.

We have demonstrated—

- (1) The correlation function in the  $E^+$  sector (V) is very close to that in free field theory. In the  $A_1^+$  sector (S) there is a significant difference at large distances, i.e., for  $z > 1/T$ . However, the magnitude of such differences are small compared to the observed fall of the correlation function by 6 orders of magnitude over the distances involved.
- (2) Both the S and V correlators are very close to the prediction of free field theory at distance less than  $T$ .
- (3) The screening mass of the V is consistent with the free field theory of overlap quarks, whereas that of the S is lighter by about 5% at the 95% confidence limit. This behavior persists into the continuum limit.
- (4) The S and V correlators in momentum space agree with free field theory of overlap quarks, after an overall normalization, only near the center of the Brillouin zone. The part with  $k_z < \pi T$  differs from free field theory for both the S and the V.
- (5) There is evidence that the screening transfer matrix does not have reflection positivity. This implies that screening in finite temperature QCD cannot be equivalent to the zero-temperature physics of a temperature dependent Hamiltonian. This statement is not controversial, since screening phenomena at finite temperature crucially involve a mixed state density matrix, whereas correlations at zero temperature involve pure quantum states.

None of these features depend upon topological nontriviality of the gauge field ensemble, since the one that has been used in these computations has vanishing topology.

## ACKNOWLEDGMENTS

This work was funded by the Indo-French Centre for the Promotion of Advanced Research under its Project No. 3104-3. These computations were performed on the Cray X1 of the Indian Lattice Gauge Theory Initiative (ILGTI) in TIFR, Mumbai.

- [1] R. V. Gai and S. Gupta, Phys. Rev. D **73**, 014004 (2006).
- [2] S. Gupta, Phys. Rev. D **64**, 034507 (2001).
- [3] S. Nadkarni, Phys. Rev. D **33**, 3738 (1986); **34**, 3904 (1986).
- [4] P. Arnold and L. G. Yaffe, Phys. Rev. D **52**, 7208 (1995).
- [5] K. Kajantie *et al.*, Phys. Rev. Lett. **79**, 3130 (1997).
- [6] S. Datta and S. Gupta, Phys. Rev. D **67**, 054503 (2003).
- [7] C. DeTar and J. Kogut, Phys. Rev. Lett. **59**, 399 (1987).
- [8] K. D. Born *et al.*, Phys. Rev. Lett. **67**, 302 (1991).
- [9] A. Gocksch *et al.*, Phys. Lett. B **205**, 334 (1988); S. Gupta, Phys. Lett. B **288**, 171 (1992).
- [10] S. Gottlieb *et al.*, Phys. Rev. Lett. **59**, 1881 (1987); Phys. Rev. D **47**, 3619 (1993); **55**, 6852 (1997); J. B. Kogut *et al.*, *ibid.* **58**, 054504 (1998).
- [11] G. Boyd *et al.*, Z. Phys. C **64**, 331 (1994); R. V. Gai and S. Gupta, Phys. Rev. Lett. **85**, 2068 (2000).
- [12] T. Hashimoto *et al.*, Nucl. Phys. **B400**, 267 (1993); Ph. de Forcrand *et al.*, Phys. Rev. D **63**, 054501 (2001); E. Laermann and P. Schmidt, Eur. Phys. J. C **20**, 541 (2001).
- [13] R. V. Gai and S. Gupta, Phys. Rev. D **67**, 034501 (2003).
- [14] S. Wissel *et al.*, Proc. Sci., LAT2005 (2006) 164.
- [15] H. Neuberger and R. Narayanan, Phys. Rev. Lett. **71**, 3251 (1993).
- [16] M. Lüscher, Phys. Lett. B **428**, 342 (1998).
- [17] R. V. Gai, S. Gupta, and R. Lacaze, Phys. Rev. D **65**, 094504 (2002).
- [18] S. Gupta, Phys. Rev. D **60**, 094505 (1999).
- [19] R. V. Gai, S. Gupta, and R. Lacaze, Proc. Sci., LAT2006 (2006) 135.
- [20] M. Hamer mesh, *Group Theory and its Application to Physical Problems* (Addison-Wesley, Reading MA, USA, 1962).
- [21] S. Datta and S. Gupta, Nucl. Phys. **B534**, 392 (1998).
- [22] H. Neuberger, Phys. Lett. B **417**, 141 (1998).
- [23] J. van den Eshof *et al.*, Comput. Phys. Commun. **146**, 203 (2002).
- [24] R. V. Gai, S. Gupta, and R. Lacaze, Comput. Phys. Commun. **154**, 143 (2003).
- [25] P. Hernandez, K. Jansen, and M. Lüscher, Nucl. Phys. **B552**, 363 (1999).